Remote forcing of the Antarctic Circumpolar Current by diapycnal mixing

D. R. Munday,[1] L. C. Allison,[2] H. L. Johnson,[3] and D. P. Marshall[1]

Received 27 January 2011; revised 1 March 2011; accepted 7 March 2011; published 22 April 2011.

[1] We show that diapycnal mixing can drive a significant Antarctic Circumpolar Current (ACC) volume transport, even when the mixing is located remotely in northern-hemisphere ocean basins. In the case of remote forcing, the globally-averaged diapycnal mixing coefficient is the important parameter. This result is anticipated from theoretical arguments and demonstrated in a global ocean circulation model. The impact of enhanced diapycnal mixing on the ACC during glacial periods is discussed. **Citation:** Munday, D. R., L. C. Allison, H. L. Johnson, and D. P. Marshall (2011), Remote forcing of the Antarctic Circumpolar Current by diapycnal mixing, *Geophys. Res. Lett.*, *38*, L08609, doi:10.1029/2011GL046849.

1. Introduction

[2] The transport of the Antarctic Circumpolar Current (ACC) is dominated by the thermal wind relative to the sea floor. Integrating the thermal wind relation across the ACC, assuming no flow at the sea floor, and neglecting variations in the Coriolis parameter, the ACC transport is:

$$T_{\mathrm{ACC}} \approx \frac{g}{\rho_0 |f_{\mathrm{ACC}}|} \int_{-H}^{0} z\,(\rho_{\mathrm{n}} - \rho_{\mathrm{s}})\,dz. \tag{1}$$

Here g is the gravitational acceleration, ρ_0 is a reference density, f_{ACC} is a typical value of the Coriolis parameter at the ACC latitude, z is depth with $z = 0$ at the surface and $z = -H$ at the sea floor, and ρ_n and ρ_s are the densities evaluated along the sloping boundaries to the north and south of Drake Passage. To the extent that isopycnals outcrop to the south, the baroclinic ACC transport is connected with the stratification to the north.

[3] Traditionally it has been assumed that the density contrast across the ACC is maintained by Southern Ocean wind and buoyancy forcing. Air-sea heat and freshwater fluxes create the density contrast and the surface wind stress generates the overturning "Deacon cell" that steepens the isopycnals. In equilibrium, this is arrested by baroclinic instability, the eddy-driven transport opposing the Deacon cell [*Danabasoglu et al.*, 1994] with the residual overturning circulation being set by surface buoyancy forcing [*Marshall*, 1997].

[4] However, the stratification to the north of the ACC is also affected by non-local processes that set the depth of the global pycnocline; these include deep water formation in the North Atlantic and diapycnal upwelling throughout the global ocean [*Gnanadesikan*, 1999; *Gnanadesikan and Hallberg*, 2000]. The link between North Atlantic deep water formation and the transport of the ACC has recently been investigated by *Fučkar and Vallis* [2007]. In this paper we explore the impact of diapycnal upwelling on the ACC transport.

[5] The idea that the ACC transport is affected by both local wind forcing over the Southern Ocean and remote diapycnal mixing is consistent with the mechanical energy budget of the ocean [*Munk and Wunsch*, 1998]. Most of the global input of wind energy (~1 TW [*Wunsch*, 2010]) occurs over the Southern Ocean. In contrast, surface buoyancy forcing provides a small global energy sink [*Wunsch and Ferrari*, 2004] (note that alternative definitions of available potential energy can lead to different conclusions [e.g., *Hughes et al.*, 2009; *Tailleux*, 2009]). Satellite altimetry suggests much of the remaining mechanical energy input (~1 TW) may be supplied by tidal dissipation in the deep ocean [*Egbert and Ray*, 2000]. To the extent that diapycnal mixing provides energy for the meridional overturning circulation of the oceans, it may also contribute to setting the ACC transport.

2. Theory

[6] A simple model of the processes that set the isopycnal slope in the Southern Ocean is that developed by *Gnanadesikan* [1999] for the global pycnocline depth. The global ocean is represented by a buoyant surface layer overlying an abyssal layer, separated by a pycnocline of depth h (Figure 1). The pycnocline depth is set by the sources and sinks of water to the surface layer:

$$T_{\mathrm{Ek}} - T_{\mathrm{Eddies}} + T_{\mathrm{U}} - T_{\mathrm{N}} = 0, \tag{2}$$

where

$$T_{\mathrm{Ek}} = \frac{\tau_{\mathrm{ACC}} L_x}{\rho_0 |f_{\mathrm{ACC}}|}, \quad T_{\mathrm{Eddies}} = \frac{\kappa_{\mathrm{GM}} L_x h}{L_y}, \quad T_{\mathrm{U}} = \frac{\int_A \kappa_{\mathrm{v}}\,dA}{h}$$

are the parameterizations suggested by *Gnanadesikan* [1999]. Thus the pycnocline depth is increased by equatorward Ekman transport in the Southern Ocean (T_{Ek}) and diapycnal upwelling (T_{U}) and decreased by poleward eddy bolus transport in the Southern Ocean (T_{Eddies}) and northern deep water formation (T_{N}). Here τ_{ACC} is the wind stress over the ACC, L_x is the circumpolar length of the ACC, κ_{GM} is the eddy diffusivity (following *Gent and McWilliams* [1990]), L_y is the meridional extent of the ACC, κ_v is the diapycnal diffusivity and A is the area of the ocean basins to the north of the ACC. Both τ_{ACC} and L_y should be calculated as

[1]Atmospheric, Oceanic and Planetary Physics, University of Oxford, Oxford, UK.
[2]Department of Meteorology, University of Reading, Reading, UK.
[3]Department of Earth Sciences, University of Oxford, Oxford, UK.

0094-8276/11/2011GL046849

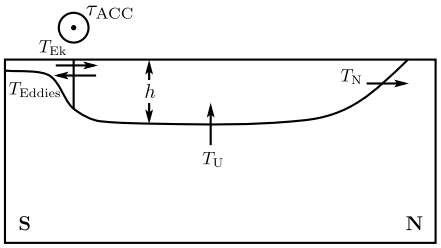

Figure 1. Schematic of the processes setting the global pycnocline depth and hence ACC transport [*Gnanadesikan*, 1999].

integrals over the ACC as described by *Allison et al.* [2010].

[7] *Gnanadesikan* [1999] further suggests parameterizing T_N as proportional to h^2. However, northern sinking also depends on subtle thermohaline feedbacks that control the meridional density gradient along the western boundary of the North Atlantic [*Johnson et al.*, 2007; *Schewe and Levermann*, 2010; *Levermann and Fürst*, 2010; also see *de Boer et al.*, 2010]. Here we sidestep these complications by treating T_N as constant.

[8] Assuming that the ACC is in geostrophic balance and that the pycnocline outcrops to the south, the ACC transport is given by

$$T_{ACC} \approx \frac{g' h^2}{2|f_{ACC}|} \tag{3}$$

where g' is the reduced gravity, analogous to (1). Thus, any process that influences the pycnocline depth will also affect the volume transport of the ACC.

[9] In order to interpret the numerical experiments described below, it is useful to consider the limiting case of no wind forcing and no deep water formation, i.e., $T_{Ek} = T_N = 0$. In this limit, the pycnocline is set by diapycnal mixing and eddies, and the ACC transport scales, through (2) and (3), as:

$$T_{ACC} \approx \frac{g' L_y \int_A \kappa_v dA}{2|f_{ACC}|\,\kappa_{GM} L_x}, \tag{4}$$

i.e., the ACC transport is linearly dependent on the amount of diapycnal mixing integrated over the basins to the north of the ACC.

[10] More generally, differentiating (2) and (3) with respect to h for fixed values of T_{Ek} and κ_{GM}, but keeping $T_N = 0$:

$$\frac{d(\ln T_{ACC})}{d\left(\ln \int_A \kappa_v dA\right)} = \frac{2T_U}{2T_U + T_{Ek}}. \tag{5}$$

This ratio asymptotes to one when diapycnal upwelling dominates over the Ekman transport and to zero when the Ekman transport dominates over diapycnal upwelling.

3. Numerical Experiments

[11] To explore the relationship between diapycnal upwelling and the ACC transport in a more realistic setting,

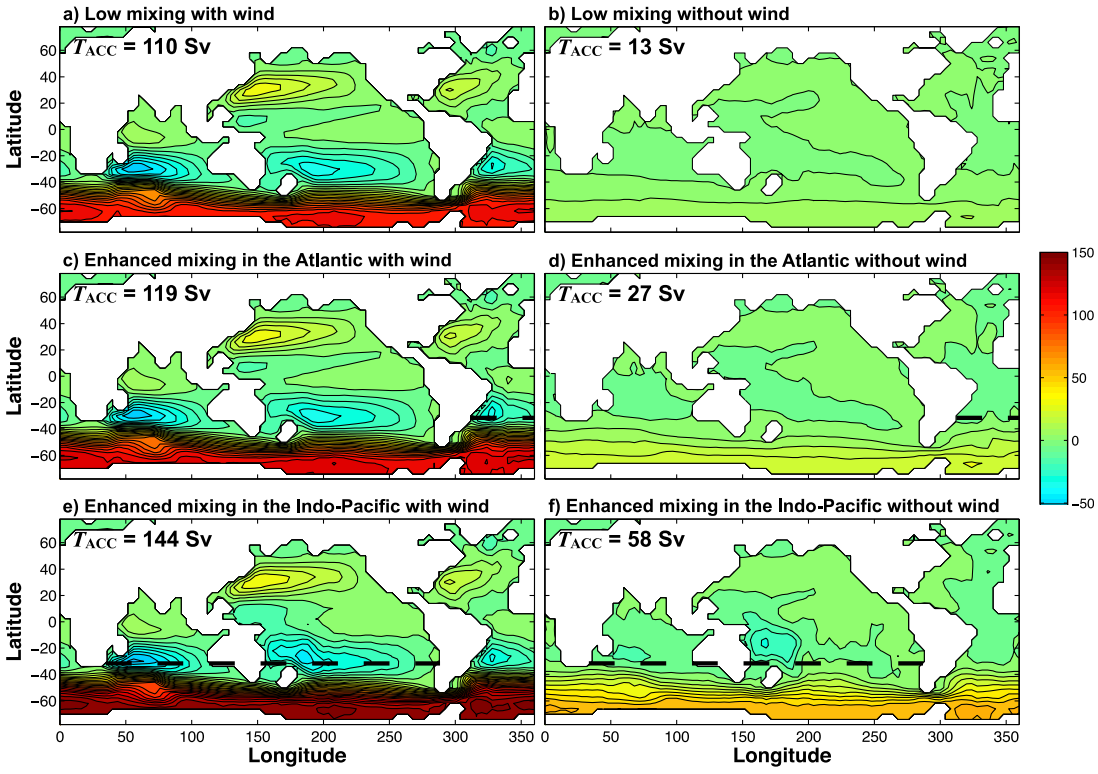

Figure 2. Depth-integrated streamfunction (Sv) at equilibrium. The ACC transport through Drake Passage is indicated in each panel. (a, b) spatially uniform low mixing of 10^{-5} m^2 s^{-1}; (c, d) enhanced mixing of 10^{-4} m^2 s^{-1} north of 32°S in the Atlantic; (e, f) enhanced mixing of 10^{-4} m^2 s^{-1} north of 32°S in the Pacific and Indian basins. (left) With and (right) without wind forcing.

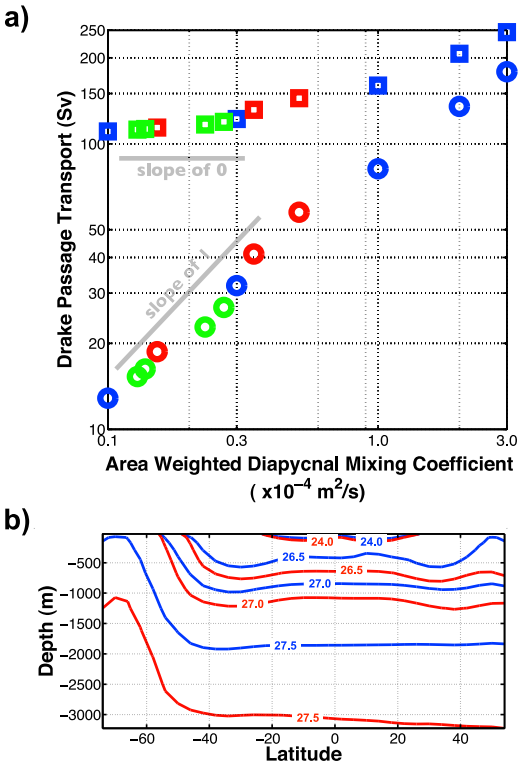

Figure 3. (a) ACC transport through Drake Passage as a function of the area-weighted diapycnal mixing coefficient $\overline{\kappa_v}$. Experiments with a spatially uniform κ_v are plotted in blue, those with enhanced mixing in the Atlantic in green, and those with enhanced mixing in the Pacific and Indian in red. Squares represent experiments with wind forcing and circles without. (b) Meridional cross-section of potential density (kgm^{-3}) in the Pacific basin at 206°E for the experiments in Figures 2a (uniform low mixing, blue) and 2e (enhanced mixing in the Pacific and Indian, red).

we now describe a series of numerical experiments with a global ocean model (MITgcm [*Marshall et al.*, 1997]). The model has horizontal grid spacing of 4° and 15 vertical levels. Mesoscale eddies are parameterized following *Gent and McWilliams* [1990] with constant isopycnal and thickness diffusivities of 1000 m^2 s^{-1}. Surface temperature and salinity are restored to climatology [*Levitus and Boyer*, 1994] over time scales of 2 and 6 months respectively, and climatological surface wind stress [*Trenberth et al.*, 1990] is applied in some experiments, each as annually-repeating seasonal cycles.

[12] Three sets of experiments are performed, each with and without surface wind stress forcing. In the first set, the diapycnal mixing coefficient (κ_v) is set to uniform values between 1×10^{-5} m^2 s^{-1} and 3.0×10^{-4} m^2 s^{-1}. In the second set, κ_v is held at 10^{-5} m^2 s^{-1} in the Southern Ocean and Atlantic, but enhanced to 10^{-4} m^2 s^{-1} in the Indian and Pacific north of: (a) 32°S, (b) the equator, and (c) 24°N. Finally, in the third set, κ_v is held at 10^{-5} m^2 s^{-1} in the Southern Ocean, Indian, and Pacific, but enhanced to 3×10^{-5} m^2 s^{-1} and 10^{-4} m^2 s^{-1} in the Atlantic north of (a) 32°S and (b) the equator.

[13] In Figure 2 we show the barotropic streamfunction at equilibrium for a subset of our experiments. Each of the calculations is presented with and without wind forcing. A comparison of Figures 2a and 2b illustrates that there is an order of magnitude increase in ACC transport due to the presence of wind forcing at the lowest, background value of κ_v. Without wind forcing, the depth-integrated gyres are absent in each of the basins but there is still a weak ACC (13 Sv).

[14] Figures 2c–2f show that enhancing diapycnal mixing by an order of magnitude in the northern basins enhances the ACC transport. When mixing is enhanced in the Atlantic, with wind forcing, the ACC transport is increased from 110 Sv to 119 Sv; enhanced mixing in the Indian and Pacific increases the ACC transport to 144 Sv.

[15] Plotted in Figure 3a is the volume transport of the ACC at Drake Passage, as a function of the area-weighted diapycnal mixing coefficient,

$$\overline{\kappa_v} = \frac{1}{A}\int_A \kappa_v dA. \tag{6}$$

To enable comparison with the theoretical prediction (5), logarithmic scales are used for both axes; the solid grey lines correspond to slopes of 0 and 1. In the absence of wind, the ACC transport varies linearly with $\overline{\kappa_v}$, as predicted by (5); this dependence weakens as $\overline{\kappa_v}$ increases due to an increase in T_N, not accounted for in the theory. In the presence of wind, the ACC transport is independent of κ_v for small values of the latter, as also predicted by (5).

[16] The dependence of ACC transport on diapycnal mixing has been noted by other authors [e.g., *Cai*, 1994; *Cai and Baines*, 1996], but attributed to interactions between baroclinicity and topography in the Southern Ocean. *Saenko et al.* [2002] also obtain a strong circumpolar transport in a coupled ocean-atmosphere model in which wind stress is not transmitted to the ocean. Figure 3b shows the model density field in the Pacific for the experiments in Figures 2a and 2e, confirming that it is the adjustment of the basinwide pycnocline that is responsible for the increase in ACC transport.

[17] In the case of altered wind forcing, the change in T_N additionally increases T_{ACC} by warming the abyss and increasing thermal shear across the ACC [*Gnanadesikan and Hallberg*, 2000]. A thermal wind calculation based on abyssal density differences (see Figures S1–S3 of the auxiliary material) suggests this effect is non-negligible, but always smaller than the values of T_{ACC} reported in Figure 3a.[1]

4. Discussion

[18] Our results suggest that diapycnal mixing, even when located in regions remote from the Southern Ocean, can drive a significant ACC transport. This is a consequence of the impact of enhanced diapycnal mixing on the global pycnocline depth, and hence on the slope of isopycnals across the ACC. Since diapycnal mixing in the deep ocean results from the dissipation of tidal energy, this implies a low-order lunar influence on the ACC transport.

[19] While the mechanical energy for an ACC forced by remote diapycnal mixing comes from tidal (and wind-driven) mixing, the momentum source is less obvious.

[1] Auxiliary materials are available in the HTML. doi:10.1029/2011GL046849.

Consider a thought experiment in which diapycnal mixing is instantaneously enhanced north of the ACC. Increased diapycnal mixing deepens the pycnocline, which is communicated globally via eastern boundary waves [*Johnson and Marshall*, 2004]. Assuming isopycnals remain pinned to the surface around Antarctica, the density gradient attempts to slump, with southward surface flow and northward flow at depth. However, the Coriolis acceleration causes these density currents to turn to their left, resulting in eastward flow at the surface and westward at depth. Finally, bottom form stress decelerates the abyssal limb, leaving an eastward ACC at the surface.

[20] During the Last Glacial Maximum (LGM), lower sea level may have led to enhanced diapycnal mixing in the abyssal ocean [*Wunsch*, 2003; *Green et al.*, 2009]. Differences are likely to have been most pronounced in the North Atlantic, where below 1000 m tidal energy dissipation may have been 3 times larger than present day [*Egbert et al.*, 2004]. Figures 2a and 2c indicate that the increase in ACC transport in our model is of order 10% when the diapycnal mixing coefficient is increased by an order of magnitude north of 32°S in the Atlantic. However, if mixing is enhanced in the Pacific and Indian basins, then the ACC transport increases by ~30%. Palaeoclimate proxy data [e.g., *Pudsey and Howe*, 1998] suggests that the ACC was indeed stronger during the LGM.

[21] The results presented in this paper are subject to the important caveat that the mesoscale eddy field in our model simulations is parameterized. Significant differences occur in model simulations when resolution is increased beyond the eddy-resolving threshold [*Hallberg and Gnanadesikan*, 2006; *Meredith and Hogg*, 2006]. On the much longer time-scales required to equilibrate the deep ocean, these differences may be more substantial. The conceptual model in Section 2 gives an indication of the competition between diapycnal mixing and mesoscale eddies. While we expect the relationship between diapycnal mixing and ACC transport to be more complicated in the presence of a fully-resolved eddy field, the basic idea that the ACC transport is sensitive to globally integrated rates of diapycnal mixing is likely to be robust.

[22] **Acknowledgments.** This study is funded by the UK Natural Environment Research Council. HLJ is supported by a Royal Society University Research Fellowship. DPM acknowledges additional support from the Oxford Martin School.

[23] The authors and Editor thank two anonymous reviewers for their assistance in evaluating this paper.

References

Allison, L. C., H. L. Johnson, D. P. Marshall, and D. R. Munday (2010), Where do winds drive the Antarctic Circumpolar Current?, *Geophys. Res. Lett.*, *37*, L12605, doi:10.1029/2010GL043355.

Cai, W. (1994), Circulation driven by observed surface thermohaline fields in a coarse resolution ocean general circulation model, *J. Geophys. Res.*, *99*, 10,163–10,181.

Cai, W., and P. G. Baines (1996), Interactions between thermohaline- and wind-driven circulations and their relevance to the dynamics of the Antarctic Circumpolar Current, in a coarse-resolution global ocean general circulation model, *J. Geophys. Res.*, *101*, 14,073–14,093.

Danabasoglu, G., J. C. McWilliams, and P. R. Gent (1994), The role of mesoscale tracer transports in the global ocean circulation, *Science*, *264*, 1123–1126.

de Boer, A. M., A. Gnanadesikan, N. R. Edwards, and A. J. Watson (2010), Meridional density gradients do not control the Atlantic overturning circulation, *J. Phys. Oceanogr.*, *40*, 368–380.

Egbert, G. D., and R. D. Ray (2000), Significant dissipation of tidal energy in the deep ocean inferred from satellite altimeter data, *Nature*, *405*, 775–778.

Egbert, G. D., R. D. Ray, and B. G. Bills (2004), Numerical modeling of the global semidiurnal tide in the present day and in the Last Glacial Maximum, *J. Geophys. Res.*, *109*, C03003, doi:10.1029/2003JC001973.

Fučkar, N. S., and G. K. Vallis (2007), Interhemispheric influence of surface buoyancy conditions on a circumpolar current, *Geophys. Res. Lett.*, *34*, L14605, doi:10.1029/2007GL030379.

Gent, P. R., and J. C. McWilliams (1990), Isopycnal mixing in ocean circulation models, *J. Phys. Oceanogr.*, *20*, 150–155.

Gnanadesikan, A. (1999), A simple predictive model for the structure of the oceanic pycnocline, *Science*, *283*, 2077–2079.

Gnanadesikan, A., and R. W. Hallberg (2000), On the relationship of the Circumpolar Current to Southern Hemisphere winds in coarse-resolution ocean models, *J. Phys. Oceanogr.*, *30*, 2013–2034.

Green, J. A. M., C. L. Green, G. R. Bigg, Tom. P. Rippeth, J. D. Scourse, and K. Uehara (2009), Tidal mixing and the meridional overturning circulation from the Last Glacial Maximum, *Geophys. Res. Lett.*, *36*, L15603, doi:10.1029/2009GL039309.

Hallberg, R., and A. Gnanadesikan (2006), The role of eddies in determining the structure and response of the wind-driven Southern Hemisphere overturning: Results from the Modeling Eddies in the Southern Ocean (MESO) project, *J. Phys. Oceanogr.*, *36*, 2232–2252.

Hughes, G. O., A. M. Hogg, and R. W. Griffiths (2009), Available potential energy and irreversible mixing in the meridional overturning circulation, *J. Phys. Oceanogr.*, *39*, 3130–3146.

Johnson, H. L., and D. P. Marshall (2004), Global teleconnections of meridional overturning circulation anomalies, *J. Phys. Oceanogr.*, *34*, 1702–1722.

Johnson, H. L., D. P. Marshall, and D. A. J. Sproson (2007), Reconciling theories of a mechanically driven meridonal overturning circulation with thermohaline forcing and multiple equilibria, *Clim. Dyn.*, *29*, 821–836.

Levermann, A., and J. J. Fürst (2010), Atlantic pycnocline theory scrutinized using a coupled climate model, *Geophys. Res. Lett.*, *37*, L14602, doi:10.1029/2010GL044180.

Levitus, S., and T. P. Boyer (1994), *World Ocean Atlas 1994, NOAA Atlas NESDIS*, NOAA, Silver Spring, Md.

Marshall, D. (1997), Subduction of water masses in an eddying ocean, *J. Mar. Res.*, *55*, 201–222.

Marshall, J., A. Adcroft, C. Hill, L. Perelman, and C. Heisey (1997), A finite volume, incompressible Navier-Stokes model for studies of the ocean on parallel computers, *J. Geophys. Res.*, *102*, 5753–5766.

Meredith, M. P., and A. M. Hogg (2006), Circumpolar response of Southern Ocean eddy activity to a change in the Southern Annular Mode, *Geophys. Res. Lett.*, *33*, L16608, doi:10.1029/2006GL026499.

Munk, W., and C. Wunsch (1998), Abyssal recipes II: Energetics of tidal and wind mixing, *Deep Sea Res., Part I*, *45*, 1977–2010.

Pudsey, C. J., and J. A. Howe (1998), Quaternary history of the Antarctic Circumpolar Current: evidence from the Scotia Sea, *Mar. Geol.*, *148*, 83–112.

Saenko, O. A., J. M. Gregory, A. J. Weaver, and M. Eby (2002), Distinguishing the influence of heat, freshwater, and momentum fluxes on ocean circulation and climate, *J. Clim.*, *15*, 3686–3697.

Schewe, J., and A. Levermann (2010), The role of meridional density differences for a wind-driven overturning circulation, *Clim. Dyn.*, *34*, 547–556.

Tailleux, R. (2009), On the energetics of stratified turbulent mixing, irreversible thermodynamics, Boussinesq models and the ocean heat engine controversy, *J. Fluid Mech.*, *638*, 339–382.

Trenberth, K. M., J. Olson, and W. G. Large (1990), The mean annual cycle in global ocean wind stress, *J. Phys. Oceanogr.*, *20*, 1742–1760.

Wunsch, C. (2003), Determining paleoceanographic circulations, with emphasis on the Last Glacial Maximum, *Quat. Sci. Rev.*, *22*, 371–385.

Wunsch, C. (2010), The work done by the wind on the oceanic general circulation, *J. Phys. Oceanogr.*, *28*, 2332–2340.

Wunsch, C., and R. Ferrari (2004), Vertical mixing, energy, and the general circulation of the oceans, *Annu. Rev. Fluid Mech.*, *36*, 281–314.

L. C. Allison, Department of Meteorology, University of Reading, Reading RG6 6BB, UK.

H. L. Johnson, Department of Earth Sciences, University of Oxford, Oxford OX1 3PR, UK.

D. P. Marshall and D. R. Munday, Atmospheric, Oceanic and Planetary Physics, Department of Physics, University of Oxford, Parks Road, Oxford OX1 3PU, UK. (munday@atm.ox.ac.uk)